Supplement to

Two years of Volatile Organic Compounds online in-situ measurements at SIRTA (Paris region, France) using Proton-Transfer-Reaction Mass Spectrometry

Leïla Simon, Valérie Gros et al

Correspondence to: Valérie Gros (valerie.gros@lsce.ipsl.fr)

Section 1: Supplementary text to the Instrumentation

Text S1: Kinetic approach for volume mixing ratio calculation using instrumental transmission

To obtain the sensitivity (in ncps/ppb) of compounds not present in the calibration standard, first the transmission of compounds present in the standard is calculated, based on the instrument's parameters and following Equation S1 (Taipale et al., 2008):

$$\frac{T_{RH^+}}{T_{H_3O^+}} = 10^9 \frac{p_{drift}}{I_{norm} p_{norm}} \frac{\mu_0 N_0}{kL} \frac{E}{N^2} S_{norm}$$

With p_{drift} being the drift pressure, I_{norm} the normalized intensity (equal to 10^6), p_{norm} the normal pressure, μ_0 being the reduced ion mobility of the primary ions and equal to 2.8 $cm^2 \cdot V^{-1} \cdot s^{-1}$, N_0 the number density of air at standard conditions, k being the reaction rate constant of the given compound (from Zhao and Zhang, 2004; Španěl et al., 1998 and 2002; Lindinger et al., 1998; if not known, a rate of $3 \cdot 10^{-9}$ is taken), L the length of the drift tube, $E=U_{drift}/L$, $N=N_A p_{drift}/(RT_{drift})$, and S_{norm} the normalized sensitivity obtained by a standard calibration.

From the transmission coefficients of calibrated m/z, a transmission curve is modelled, from which the transmission coefficients of the other m/z are extracted and used to retrieve the sensitivity (S_{norm}) using a reversed equation of (S1).

Text S2: Concentration calculation from volume mixing ratios (VMR)

The results in this paper are expressed in concentrations ($\mu g \cdot m^{-3}$), calculated from the VMR (ppb) following Equation S2:

$$Concentration = VMR \cdot \frac{M}{V_{air} \frac{T_{atm}}{T_0} \frac{P_0}{P_{atm}}}$$

With M the molar mass of the compound, V_{air} the standard volume of air equal to 22.41 L, T_{atm} the atmospheric temperature in K, T_0 the standard temperature of 273.15 K, P_0 the standard atmospheric pressure of 1 013.25 hPa, and P_{atm} the atmospheric pressure in hPa.

Text S3: Discussion for tentative attribution of the measured m/z, based on PTR-ToF-MS measurements and the literature

m/z 31 mostly corresponds to CH_2O (formaldehyde), which cannot be precisely quantified by PTR-MS, due to its proton affinity being too close to that of water, and is thus defined as its proxy. *m/z 33* corresponds to CH_3OH (methanol), the main alcohol present in the atmosphere, and is also the most important oxygenated VOC; although at this mass there are interferences from O_2^+, thus resulting in a high background. *At m/z 42,* CH_3CN (acetonitrile) is the main compound measured; interferences from other compounds are negligible (Yuan et al., 2017b). Acetaldehyde is the main component detected at *m/z 45,* for which the main source is biomass burning. *m/z 46* can correspond to several compounds: it was mostly identified as CH_3NO and C_2H_7N, respectively formamide and dimethylamine, both compounds emitted by agricultural activities (Yuan et al., 2017a; Kammer et al., 2019). However, a few studies reported this mass as NO_2^+, that would correspond notably to peroxyacetyl nitrate (PAN) fragmentations (Yuan et al., 2017b) or other organic nitrates (Aoki et al., 2007; Duncianu et al., 2017), but cannot be precisely quantify using H_3O^+ ionization. In this study, we will refer to it as m/z 46 (or m46). *m/z 47* corresponds to C_2H_6O (ethanol) and CH_2O_2 (formic acid) and will therefore be referred to as their sum, although the sensitivity of ethanol is lower than that of formic acid. Their seasonal contribution can be found in Table 2, and shows that *m/z 47* is dominated by formic acid in spring and summer (> 90%), but in autumn and winter, ethanol contribution becomes significant. This is a similar trend to that of furan's and isoprene's contributions to m/z 69. *m/z 57* is usually attributed to propenal (C_3H_4O) (Knighton et al., 2007; Languille et al., 2020), but there are interferences from C_4H_8: butenes or other hydrocarbons' fragmentations, that cannot be precisely quantified but seem to be dominant in our study (Table 2). *m/z 58* corresponds to allylamine, a compound emitted by agricultural activities (Kammer et al., 2019). *m/z 59* could be correspond to C_3H_6O (acetone + propanal), C_4H_{10} (butane) and $C_2H_2O_2$ (glyoxal); PTR-ToF-MS measurements showed that in all seasons, C_3H_6O is dominant by about 97%. de Gouw and Warneke (2007) indicated that propanal is also negligible and *m/z 59* can be regarded as acetone only. *m/z 60* corresponds mainly to trimethylamine, which is mostly emitted by agricultural activities (Kammer et al., 2019). *m/z 61* is attributed to acetic acid, an agricultural and biogenic compound. *m/z 63* corresponds to dimethylsulfide, emitted by phytoplanktonic activities in the oceans. *m/z 69* corresponds to C_4H_4O: furan and C_5H_8: isoprene and fragments of methylbutenol (MBO), but PTR-ToF-MS measurements showed that MBO is negligible (see discussion of *m/z 87*). Furan is emitted by biomass-burning activities and has highest contributions in autumn and winter; while in spring and summer, m/z 69 can be almost exclusively attributed to isoprene, due to its important biogenic source, although it can also be emitted by anthropogenic sources (Borbon et al., 2001; Wagner and Kuttler, 2014; Panopoulou, 2020). *m/z 71* corresponds mainly (by about 85%) to C_4H_6O, the sum of methyl vinyl ketone (MVK), methacrolein (MACR), ISOPOOH, and crotonaldehyde. ISOPOOH are formed from isoprene oxidation under low NO_X conditions (Surratt et al., 2010; Budisulistiorini et al., 2013), and so are expected to be low in a suburban area. In summer, MVK + MACR would be dominant as they are the main isoprene oxidation products, and crotonaldehyde might dominate *m/z 71* in winter, due to its wood burning source (Lipari et al., 1984; Languille et al., 2020). Due to its overall higher level in summer, this m/z will be considered as MVK + MACR. *m/z 73* is mainly attributed to methyl ethyl ketone (MEK) in ambient air (Yuan et al., 2017b). *m/z 75* was identified as $C_3H_6O_2$

(methylacetate, hydroxyacetone, propanoic acid); methylacetate would be a biomass burning compound (Bruns et al., 2017), while hydroxyacetone and propanoic acid are of biogenic origins (Yuan et al., 2017b). It is not possible to separate these compounds because they are isomers, but methylacetate is expected to be the dominant VOC in winter and hydroxyacetone + propanoic acid to be dominant in summer. *m/z 79* corresponds to benzene (C_6H_6). *m/z 81* corresponds to fragments of monoterpenes (mostly) and of PAHs. *m/z 83* was identified as methylfuran (C_5H_6O), that can be found in biomass burning plumes (Bruns et al., 2016), and as a minor oxidation product of isoprene (Kroll et al., 2006; and references therein). This mass was also identified as C_6H_{10}, fragments of hydrocarbons (HC) from gasoline and diesel cars (Gueneron et al., 2015). In winter and autumn, methylfuran is dominant (Table 2) while C_6H_{10} is significant in spring and summer. *m/z 85* mainly corresponds to methylbutenone (C_5H_8O), identified as a biomass burning compound, by (Bruns et al., 2017) and as a biogenic compound by Kroll et al. (2006). *m/z 87* corresponds to $C_4H_6O_2$ (butanedione + methacrylic acid) and $C_5H_{10}O$ (methylbutenol, MBO). Butanedione was found in biomass burning plumes (Bruns et al., 2017), methacrylic acid was identified as an isoprene oxidation product (Williams et al., 2001; Nguyen, 2012) and MBO was shown to be emitted by biogenic sources (Holzinger et al, 2005; Kim et al., 2010). PTR-ToF-MS measurements showed that $C_4H_6O_2$ is dominant (> 80%), thus butanedione would be the main compound in winter and methacrylic acid (MAA) in summer. *m/z 93* corresponds to toluene (C_7H_8), a major traffic compound. *m/z 97* can be attributed to several compounds such as C_2-substituted furans and furaldehydes (Yuan et al., 2017b), but Bruns et al. (2017) reported this mass as furfural ($C_5H_4O_2$) in biomass-burning influenced regions, and Languille et al. (2020) also defined m/z 97 as furfural in winter at SIRTA. *m/z 99* was identified as $C_5H_6O_2$ (furfuryl alcohol) by (Stockwell et al., 2015), and as $C_4H_2O_3$ (furandione) by Bruns et al. (2017), both present in aged biomass burning plumes. In this study, both compounds are present so this mass will be regarded as their sum. *m/z 107* corresponds to C_8H_{10} (C_8-aromatics: xylenes, ethylbenzene) and C_7H_6O (benzaldehyde); C_8-aromatics are dominant by about 80% (Table 2), and thus this mass will be regarded as mainly C_8-aromatics. *m/z 111* was identified as benzenediol by Bruns et al. (2016) as a biomass burning compound. *m/z 121* corresponds to C_9-aromatics (trimethylbenzenes), mainly emitted by traffic. *m/z 137* corresponds to monoterpenes, for which the main source is supposed to be biogenic, although anthropogenic sources, traffic and wood burning, were identified recently (Panopoulou et al., 2020). *m/z 139* corresponds to nopinone, an oxidation product of monoterpenes. *m/z 147* corresponds to dichlorobenzene. *m/z 151* is identified as $C_9H_{10}O_2$, pinonaldehyde, an alpha-pinene ozonolysis product. Pinonaldehyde is measured at m/z 169 and at m/z 151, which corresponds to pinonaldehyde-H_2O.

Section 2: Tables and Figures

Table S1: Instrument parameters throughout the two-year measurement period

Name	Symbol	Value (unit)
Pressure in the drift chamber	P_{drift}	2.2 mbar
Temperature in the drift chamber	T_{drift}	40 °C
Temperature in the inlet tube	T_{inlet}	40 °C
Voltage in the drift chamber	U_{drift}	600 V
Water flow	F_{H2O}	5–8 mL·min^{-1}
Voltage	U_{SO}	90–130 V
Voltage	U_S	80–120 V
Source intensity	I_{hc}	3–6 mA
Voltage in the SEM	U_{SEM}	2000–3500 V
Drift tube length	L	9.2 cm
Collision energy	E/N	134.4 Td

90

Table S2: Standard canisters used for calibration throughout the two-year measurement period

Start	End	Reference of standard	Composition	VMR
1/18/2020	9/10/2020	R0904, Ionicon Analytik	Methanol, Acetonitrile, Acetaldehyde, Acrolein, Acetone, Isoprene, Crotonaldehyde, 2-Butanone, Benzene, Toluene, o-Xylene, α-pinene, 1,2-Dichlorobenzene	1 ppm
9/10/2020	6/15/2021	L5387, Ionicon Analytik	Methanol, Acetonitrile, Acetone, Isoprene, Benzene, Toluene, Xylenes, Trimethylbenzene, 1,2-Dichlorobenzene	100 ppb
9/1/2021	12/31/2021	D155286, SIAD	Methanol, Acetonitrile, Acetaldehyde, Acrolein, Acetone, MEK, Benzene, Toluene, o-Xylene, α-pinene, 1,2-Dichlorobenzene	1 ppm

95

Table S3: Descriptive statistics obtained for 2020 and 2021. Values are in µg·m^{-3}

	Mean 2020	Median 2020	25th percentile 2020	75th percentile 2020	sigma 2020	Mean 2021	Median 2021	25th percentile 2021	75th percentile 2021	sigma 2021
Methanol	3.90	2.78	1.30	5.18	3.89	3.90	2.81	1.74	4.70	3.51
Acetone	2.61	2.05	1.19	3.23	2.10	2.30	1.71	1.10	2.97	1.81
Acetic acid	1.72	1.03	0.55	2.12	1.92	1.47	1.10	0.57	2.02	1.28
Acetaldehyde	1.09	0.78	0.48	1.38	0.94	1.13	0.94	0.57	1.49	0.85
Ethanol + Formic acid	0.96	0.62	0.32	1.18	1.06	0.95	0.78	0.52	1.23	0.71
MEK	0.58	0.42	0.26	0.73	0.53	0.55	0.45	0.26	0.72	0.47
Butandione + MAA	0.21	0.14	-0.12	0.41	0.45	0.33	0.28	0.08	0.53	0.37
m75 – $C_3H_6O_2$	0.36	0.23	0.14	0.44	0.39	0.31	0.25	0.14	0.41	0.24
Pinonaldehyde	0.40	0.34	0.17	0.64	0.44	0.17	0.08	-0.01	0.25	0.41
MVK+MACR	0.39	0.19	0.08	0.44	0.56	0.18	0.12	0.06	0.21	0.21
Methylfuran + C_6H_{10}	0.21	0.14	0.09	0.24	0.22	0.31	0.25	0.14	0.41	0.17
Furfural	0.21	0.13	0.07	0.24	0.26	0.19	0.12	0.06	0.24	0.21
Furandione + furfuryl alcohol	0.18	0.12	0.08	0.22	0.15	0.14	0.12	0.07	0.19	0.11
Formaldehyde proxy	0.15	0.12	0.04	0.21	0.16	0.12	0.12	0.04	0.21	0.15
Nopinone	0.17	0.15	0.04	0.28	0.22	0.07	0.05	0.01	0.12	0.19
Benzenediol	0.16	0.13	0.07	0.21	0.17	0.12	0.09	0.03	0.18	0.16
Methylbutenone	0.10	0.07	0.04	0.13	0.10	0.10	0.08	0.04	0.13	0.09
Toluene	0.65	0.39	0.22	0.74	0.77	0.69	0.48	0.27	0.87	0.65
C8_Aromatics	0.62	0.36	0.18	0.72	0.86	0.61	0.40	0.20	0.79	0.66
Benzene	0.42	0.32	0.16	0.53	0.42	0.50	0.42	0.28	0.65	0.36
C9_Aromatics	0.62	0.36	0.18	0.72	0.49	0.46	0.31	0.18	0.57	0.55
Isoprene + Furan	0.70	0.45	0.22	0.85	0.89	0.45	0.33	0.19	0.55	0.44
C_4H_8 + Propenal	0.60	0.43	0.27	0.74	0.57	0.81	0.60	0.33	1.06	0.84
Monoterpenes	0.57	0.42	0.23	0.75	0.85	0.42	0.30	0.18	0.50	0.59
Monoterpenes frag	0.18	0.14	0.10	0.20	0.22	0.20	0.15	0.11	0.20	0.21
m46	1.00	0.34	0.05	1.09	1.94	0.94	0.38	0.08	1.06	1.45
Trimethylamine	0.17	0.15	0.09	0.21	0.13	0.15	0.12	0.08	0.19	0.11
Acetonitrile	0.14	0.13	0.09	0.18	0.08	0.16	0.13	0.09	0.21	0.12
Allylamine	0.04	0.04	0.02	0.05	0.03	0.05	0.04	0.02	0.06	0.05
DMS	0.04	0.04	0.00	0.08	0.07	0.06	0.06	0.03	0.09	0.06
Dichlorobenzene	0.17	0.12	0.05	0.31	0.28	0.05	0.04	-0.03	0.12	0.18
TOTAL	19.11	14.52	8.46	24.09	15.91	17.65	14.49	9.33	23.31	12.71

100

Table S4: Mean VOC concentrations (µg·m^{-3}) per cluster

	Continental	Anticyclonic	Oceanic_1	Oceanic_2	North_1	North_2
Formaldehyde proxy	0.22	0.18	0.04	0.09	0.18	0.11
Methanol	6.21	5.41	2.23	2.74	4.31	2.31
Acetonitrile	0.21	0.18	0.12	0.12	0.17	0.11
Acetaldehyde	1.97	1.41	0.53	0.74	1.39	0.88
mz_46	2.84	1.10	0.09	0.35	1.58	0.95
Ethanol + Formic acid	1.70	1.16	0.47	0.66	1.22	0.74
C_4H_8 + Propenal	0.97	0.86	0.44	0.49	0.94	0.62
Allylamine	0.06	0.05	0.03	0.03	0.05	0.04
Acetone	4.03	3.22	1.53	1.74	2.82	1.55
Trimethylamine	0.25	0.22	0.11	0.11	0.18	0.11
Acetic acid	3.17	2.11	0.64	0.99	1.98	1.24
DMS	0.07	0.07	0.04	0.04	0.06	0.04
Isoprene + Furan	0.81	0.88	0.41	0.42	0.58	0.32
MVK + MACR	0.46	0.43	0.18	0.21	0.29	0.12
MEK	0.97	0.75	0.30	0.37	0.71	0.45
m75 – $C_3H_6O_2$	0.61	0.48	0.17	0.20	0.39	0.25
Benzene	0.76	0.55	0.28	0.32	0.53	0.43
Monoterpenes frag	0.23	0.25	0.14	0.14	0.23	0.14
Methylfuran + C_6H_{10}	0.28	0.28	0.12	0.13	0.23	0.15
Methylbutenone	0.14	0.14	0.06	0.07	0.12	0.09
Butanedione + MAA	0.52	0.44	-0.01	0.10	0.42	0.18
Toluene	1.11	0.87	0.32	0.44	0.90	0.50
Furfural	0.29	0.27	0.13	0.14	0.22	0.16
Furandione + furfuryl alcohol	0.24	0.21	0.10	0.11	0.18	0.14
C8-Aromatics	1.06	0.82	0.27	0.39	0.85	0.47
Benzenediol	0.21	0.19	0.09	0.11	0.18	0.13
C9-Aromatics	0.63	0.53	0.24	0.30	0.64	0.38
Monoterpenes	0.61	0.74	0.38	0.37	0.53	0.36
Nopinone	0.20	0.19	0.10	0.07	0.11	0.12
Dichlorobenzene	0.14	0.15	0.08	0.11	0.11	0.12
Pinonaldehyde	0.38	0.36	0.24	0.26	0.26	0.32

Table S5: Correlations of VOCs with external tracers in winter

TRAFFIC WINTERS	R^2	WOOD BURNING WINTERS	R^2	MONOTERPENES WINTERS	R^2
m93xBCff	0.73	m83xBCwb	0.88	m137xm97	0.231
m107xBCff	0.80	m85xBCwb	0.83	m137xBCff	0.302
m121xBCff	0.77	m87xBCwb	0.53	m137xNO2	0.234
m93xNO2	0.65	m97xBCwb	0.75	m137xm93	0.404
m107xNO2	0.64	m99xBCwb	0.74	m137xm107	0.374
m121xNO2	0.61	m111xBCwb	0.67	m137xm121	0.24
m93xm107	0.85			m81xm97	0.347
m93xm121	0.64			m81xBCff	0.431
m107xm121	0.58			m81xNO2	0.371
				m81xm93	0.593
				m81xm107	0.523
				m81xm121	0.530

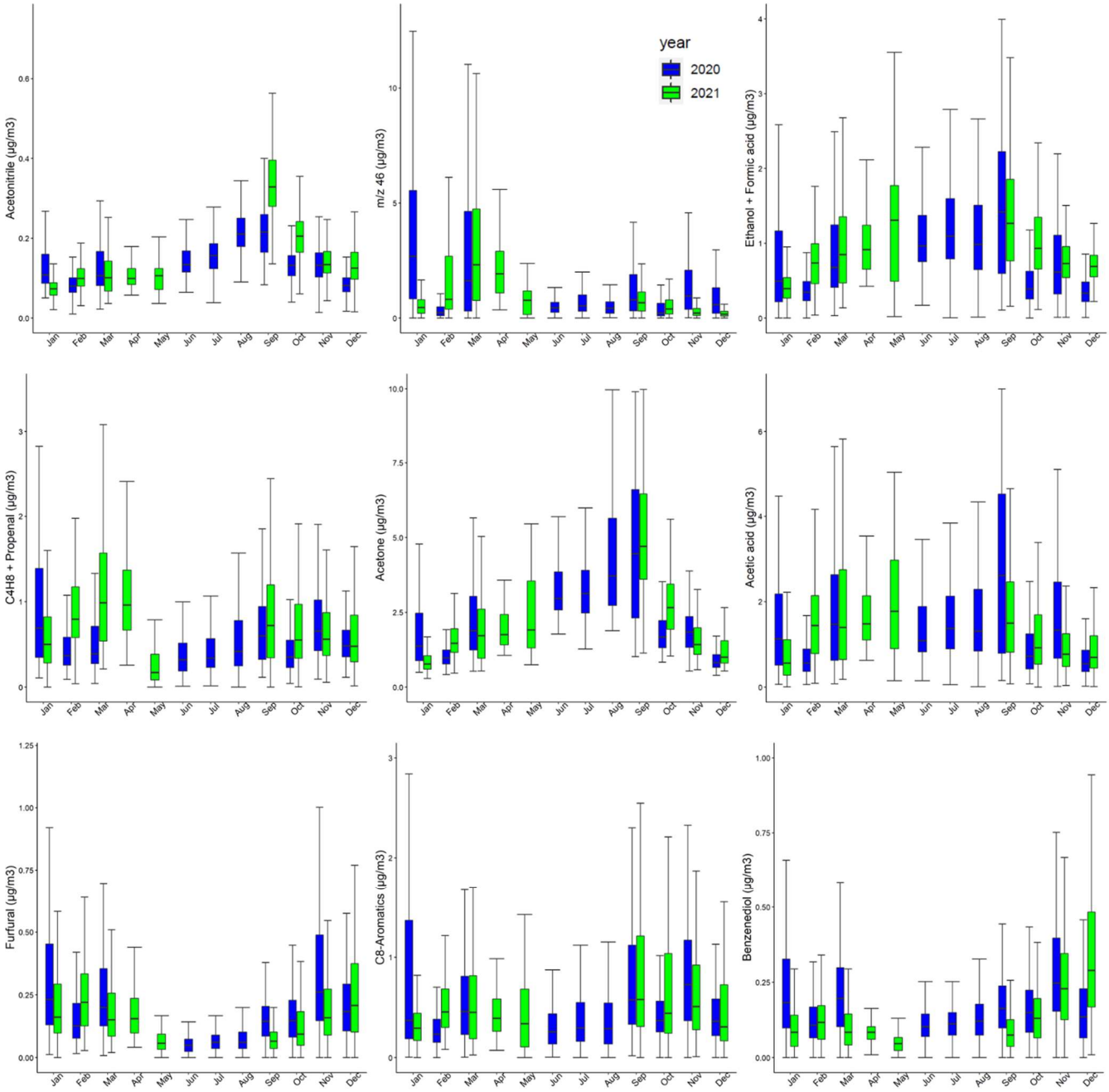

Figure S1: Monthly distribution of Furfural (m/z 97) for 2020 (blue) and 2021 (green). Boxes represent 25th and 75th percentiles, the line is the median. Whiskers represent 5th and 95th percentiles

References

Aoki, N., Inomata, S., and Tanimoto, H.: Detection of C1–C5 alkyl nitrates by proton transfer reaction time-of-flight mass spectrometry, International Journal of Mass Spectrometry, 263, 12–21, https://doi.org/10.1016/j.ijms.2006.11.018, 2007.

Borbon, A., Fontaine, H., Veillerot, M., Locoge, N., Galloo, J. C., and Guillermo, R.: An investigation into the traffic-related fraction of isoprene at an urban location, Atmospheric Environment, 35, 3749–3760, https://doi.org/10.1016/S1352-2310(01)00170-4, 2001.

Bruns, E. A., El Haddad, I., Slowik, J. G., Kilic, D., Klein, F., Baltensperger, U., and Prévôt, A. S. H.: Identification of significant precursor gases of secondary organic aerosols from residential wood combustion, Sci Rep, 6, 27881, https://doi.org/10.1038/srep27881, 2016.

Bruns, E. A., Slowik, J. G., El Haddad, I., Kilic, D., Klein, F., Dommen, J., Temime-Roussel, B., Marchand, N., Baltensperger, U., and Prévôt, A. S. H.: Characterization of gas-phase organics using proton transfer reaction time-of-flight mass spectrometry: fresh and aged residential wood combustion emissions, Atmos. Chem. Phys., 17, 705–720, https://doi.org/10.5194/acp-17-705-2017, 2017.

Budisulistiorini, S. H., Canagaratna, M. R., Croteau, P. L., Marth, W. J., Baumann, K., Edgerton, E. S., Shaw, S. L., Knipping, E. M., Worsnop, D. R., Jayne, J. T., Gold, A., and Surratt, J. D.: Real-Time Continuous Characterization of Secondary Organic Aerosol Derived from Isoprene Epoxydiols in Downtown Atlanta, Georgia, Using the Aerodyne Aerosol Chemical Speciation Monitor, Environ. Sci. Technol., 47, 5686–5694, https://doi.org/10.1021/es400023n, 2013.

Duncianu, M., David, M., Kartigueyane, S., Cirtog, M., Doussin, J.-F., and Picquet-Varrault, B.: Measurement of alkyl and multifunctional organic nitrates by proton-transfer-reaction mass spectrometry, Atmos. Meas. Tech., 10, 1445–1463, https://doi.org/10.5194/amt-10-1445-2017, 2017.

de Gouw, J. and Warneke, C.: Measurements of volatile organic compounds in the earth's atmosphere using proton-transfer-reaction mass spectrometry, Mass Spectrom. Rev., 26, 223–257, https://doi.org/10.1002/mas.20119, 2007.

Gueneron, M., Erickson, M. H., VanderSchelden, G. S., and Jobson, B. T.: PTR-MS fragmentation patterns of gasoline hydrocarbons, International Journal of Mass Spectrometry, 379, 97–109, https://doi.org/10.1016/j.ijms.2015.01.001, 2015.

Holzinger, R., Lee, A., Paw U, K T, and Goldstein, A. H.: Observations of oxidation products above a forest imply biogenic emissions of very reactive compounds, Atmos. Chem. Phys., 9, 2005.

Kammer, J., Décuq, C., Baisnée, D., Ciuraru, R., Lafouge, F., Buysse, P., Bsaibes, S., Henderson, B., Cristescu, S. M., Benabdallah, R., Chandra, V., Durand, B., Fanucci, O., Petit, J.-E., Truong, F., Bonnaire, N., Sarda-Estève, R., Gros, V., and Loubet, B.: Characterization of particulate and gaseous pollutants from a French dairy and sheep farm, Science of The Total Environment, 135598, https://doi.org/10.1016/j.scitotenv.2019.135598, 2019.

Kim, S., Karl, T., Guenther, A., Tyndall, G., Orlando, J., Harley, P., Rasmussen, R., and Apel, E.: Emissions and ambient distributions of Biogenic Volatile Organic Compounds (BVOC) in a ponderosa pine ecosystem: interpretation of PTR-MS mass spectra, Atmos. Chem. Phys., 13, 2010.

Knighton, W. B., Herndon, S. C., Shorter, J. H., Miake-Lye, R. C., Zahniser, M. S., Akiyama, K., Shimono, A., Kitasaka, K., Shimajiri, H., and Sugihara, K.: Laboratory Evaluation of an Aldehyde Scrubber System Specifically for the Detection of Acrolein, Journal of the Air & Waste Management Association, 57, 1370–1378, https://doi.org/10.3155/1047-3289.57.11.1370, 2007.

Kroll, J. H., Ng, N. L., Murphy, S. M., Flagan, R. C., and Seinfeld, J. H.: Secondary Organic Aerosol Formation from Isoprene Photooxidation, Environ. Sci. Technol., 40, 1869–1877, https://doi.org/10.1021/es0524301, 2006.

Languille, B., Gros, V., Petit, J.-E., Honoré, C., Baudic, A., Perrussel, O., Foret, G., Michoud, V., Truong, F., Bonnaire, N., Sarda-Estève, R., Delmotte, M., Feron, A., Maisonneuve, F., Gaimoz, C., Formenti, P., Kotthaus, S., Haeffelin, M., and Favez, O.: Wood burning: A major source of Volatile Organic Compounds during wintertime in the Paris region, Science of The Total Environment, 711, 135055, https://doi.org/10.1016/j.scitotenv.2019.135055, 2020.

Lindinger, W., Jordan, A., and Hansel, A: Proton-transfer-reaction mass spectrometry (PTR–MS): on-line monitoring of volatile organic compounds at pptv levels, Chem. Soc. Rev., 27, 347, https://doi.org/10.1039/a827347z, 1998.

Lipari, Frank., Dasch, J. M., and Scruggs, W. F.: Aldehyde emissions from wood-burning fireplaces, Environ. Sci. Technol., 18, 326–330, https://doi.org/10.1021/es00123a007, 1984.

Panopoulou, A.: Yearlong measurements of monoterpenes and isoprene in a Mediterranean city (Athens): Natural vs anthropogenic origin, Atmospheric Environment, 12, 2020.

Panopoulou, A., Liakakou, E., Sauvage, S., Gros, V., Locoge, N., Stavroulas, I., Bonsang, B., Gerasopoulos, E., and Mihalopoulos, N.: Yearlong measurements of monoterpenes and isoprene in a Mediterranean city (Athens): Natural vs anthropogenic origin, Atmospheric Environment, 243, 117803, https://doi.org/10.1016/j.atmosenv.2020.117803, 2020.

Španěl, P., Wang, T., and Smith, D.: A selected ion flow tube, SIFT, study of the reactions of H3O+, NO+ and O2+ ions with a series of diols, International Journal of Mass Spectrometry, 218, 227–236, https://doi.org/10.1016/S1387-3806(02)00724-8, 2002.

Stockwell, C. E., Veres, P. R., Williams, J., and Yokelson, R. J.: Characterization of biomass burning emissions from cooking fires, peat, crop residue, and other fuels with high-resolution proton-transfer-reaction time-of-flight mass spectrometry, Atmos. Chem. Phys., 15, 845–865, https://doi.org/10.5194/acp-15-845-2015, 2015.

Surratt, J. D., Chan, A. W. H., Eddingsaas, N. C., Chan, M., Loza, C. L., Kwan, A. J., Hersey, S. P., Flagan, R. C., Wennberg, P. O., and Seinfeld, J. H.: Reactive intermediates revealed in secondary organic aerosol formation from isoprene, Proceedings of the National Academy of Sciences, 107, 6640–6645, https://doi.org/10.1073/pnas.0911114107, 2010.

Taipale, R., Ruuskanen, T. M., Rinne, J., Kajos, M. K., Hakola, H., Pohja, T., and Kulmala, M.: Technical Note: Quantitative long-term measurements of VOC concentrations by PTR-MS – measurement, calibration, and volume mixing ratio calculation methods, Atmos. Chem. Phys., 18, 2008.

Wagner, P. and Kuttler, W.: Biogenic and anthropogenic isoprene in the near-surface urban atmosphere — A case study in Essen, Germany, Science of The Total Environment, 475, 104–115, https://doi.org/10.1016/j.scitotenv.2013.12.026, 2014.

Williams, J., Pöschl, U., Crutzen, P. J., Hansel, A., Holzinger, R., Warneke, C., Lindinger, W., and Lelieveld, J.: An Atmospheric Chemistry Interpretation of Mass Scans Obtained from a Proton Transfer Mass Spectrometer Flown over the Tropical Rainforest of Surinam, 34, n.d.

Yuan, B., Coggon, M. M., Koss, A. R., Warneke, C., Eilerman, S., Peischl, J., Aikin, K. C., Ryerson, T. B., and de Gouw, J. A.: Emissions of volatile organic compounds (VOCs) from concentrated animal feeding operations (CAFOs): chemical compositions and separation of sources, Atmos. Chem. Phys., 17, 4945–4956, https://doi.org/10.5194/acp-17-4945-2017, 2017a.

Yuan, B., Koss, A. R., Warneke, C., Coggon, M., and Sekimoto, K.: Proton-Transfer-Reaction Mass Spectrometry: Applications in Atmospheric Sciences, Chem. Rev., 43, 2017b.

Zhao, J. and Zhang, R.: Proton transfer reaction rate constants between hydronium ion (H3O+) and volatile organic compounds, Atmospheric Environment, 38, 2177–2185, https://doi.org/10.1016/j.atmosenv.2004.01.019, 2004.